

High transparent polyimides containing pyridine and biphenyl units: Synthesis, thermal, mechanical, crystal and optical properties



Yue Guan, Chunbo Wang, Daming Wang, Guodong Dang, Chunhai Chen, Hongwei Zhou, Xiaogang Zhao*

Alan G. MacDiarmid Institute, Jilin University, Changchun 130012, PR China

ARTICLE INFO

Article history:

Received 5 November 2014

Received in revised form

7 January 2015

Accepted 4 February 2015

Available online 17 February 2015

Keywords:

Polyimide synthesis

Biphenyl structure

Pyridine diamine

ABSTRACT

Two series of isomeric pyridine-containing aromatic diamine monomers, 2,2'-bis(5-amino-2-pyridinoxy)biphenyl (2a), 4,4'-bis(5-amino-2-pyridinoxy)biphenyl (2b), and 4,4'-bis(5-amino-6-methyl-2-pyridinoxy)biphenyl (2c), 4,4'-bis(5-amino-3-methyl-2-pyridinoxy)biphenyl (2d), 4,4'-bis(5-amino-4-methyl-2-pyridinoxy)biphenyl (2e) were successfully synthesized. Aimed at clarifying the structure-property relationships of containing pyridine and biphenyl high-performance polymers, polyimides PI-(1–5) were synthesized via a two-step thermal imidization derived from 2b and various commercially aromatic anhydrides and polyimide PI-(6–9) was synthesized derived from 2,2'-bis(3,4-dicarboxyphenyl) hexafluoropropane dianhydride (6FDA) and 2a, 2c, 2d and 2e. Furthermore, comparative studies on their properties including solubility, thermal and mechanical, optical properties, and crystalline were thoroughly performed. Some property differences of the isomers caused by the sequence changes were found.

© 2015 Elsevier Ltd. All rights reserved.

1. Introduction

Over many years, with the fast development of different high-tech fields, the performances of the polymer materials are simultaneously put forward to high requirements. As the most successful classes of high temperature polymers, polyimides have been shown to be excellent comprehensive performance and their applications are growing steadily. Polyimides have excellent mechanical properties such as high mechanical strength and excellent electrical properties, high thermal stability as well as good chemical resistance [1–5]. Therefore, polyimides have been widely employed in the fields of the aerospace, microelectronics, coatings, functional membranes, etc. [6–9]. Many studies of new polyimide synthesis have been focused on the preparation of novel diamine or dianhydride having a special structure, such as high fluoride content structure [10], high sulfur content structure [11], high symmetrical structure and unsymmetrical structure [12], triphenylamine-based structure [13], neighboring tetrahedral unit structure [14], etc. Compounds having a biphenyl structures, possess high

symmetrical structure and have been receiving more attention as a monomer for the synthesis of novel polyimide.

In the high-performance polymer materials, the molecular chain comprising biphenylene may effectively change some properties of the polymer, resulting in high crystallinity, thermal stability, mechanical properties, but low solubility [15]. Low solubility of the polyimide affects processing and limits its application. Solubility of the polyimides has been targeted by several methods, such as introduction of flexible linkages [16–18], bulky pendent substituents [19–21], or aromatic heterocyclic [22–24]. The methyl-substituted pyridine or pyridine is introduced into a containing biphenyl structure diamine for the synthesis of the polyimide can effectively improve its solubility and processability while not deteriorating positive properties.

In this article, for investigating the structure-property relations of isomeric PIs, two series of novel isomeric diamine monomers, 2,2'-bis(5-amino-2-pyridinoxy)biphenyl (2a), 4,4'-bis(5-amino-2-pyridinoxy)biphenyl (2b), and 4,4'-bis(5-amino-6-methyl-2-pyridinoxy)biphenyl (2c), 4,4'-bis(5-amino-3-methyl-2-pyridinoxy)biphenyl (2d), 4,4'-bis(5-amino-4-methyl-2-pyridinoxy)biphenyl (2e) were synthesized to prepare polyimides. Direct property comparisons of these isomeric PIs were exhibited, including solubility, thermal, crystal, mechanical and optical properties.

* Corresponding author. Tel./fax: +86 431 85168335.

E-mail addresses: guanyue200888@163.com (Y. Guan), xiaogang@jlu.edu.cn (X. Zhao).

2. Experimentation

2.1. Materials

4,4'-Dihydroxybiphenyl, 2,2'-dihydroxybiphenyl, 2-chloro-5-nitropyridine, 2-chloro-3-methyl-5-nitropyridine, 2-chloro-4-methyl-5-nitropyridine and 6-chloro-2-methyl-3-nitropyridine were purchased from J&K Chemical Co., Ltd. Pyromellitic dianhydride (PMDA), 3,3',4,4'-Biphenyltetracarboxylic dianhydride (BPDA), 3,3',4,4'-oxydiphthalic anhydride (ODPA), 3,3',4,4'-Benzophenonetetracarboxylic dianhydride (BTDA), and 2,2'-bis(3,4-dicarboxyphenyl) hexafluoropropane dianhydride (6FDA) were supplied by Sinopharm Chemical Reagent Beijing Co. Ltd, and these aromatic dianhydrides were all recrystallized from acetic anhydride and then dried in vacuum at 150 °C for 10 h. 10% Palladium on charcoal (Pd/C) was purchased from Acros. *N,N*-dimethylformamide (DMF), *N,N*-dimethylacetamide (DMAc) were purified by distillation under reduced pressure over CaH₂ and stored over 4 Å molecular sieves. The other commercially available reagents and solvents were used without further purification.

2.2. Measurements

The ¹H NMR and ¹³C NMR spectra were recorded on a BRUKER-300 spectrometer at 300 or 75 MHz in deuterated chloroform (CDCl₃) or dimethyl sulfoxide (DMSO-d₆). FT-IR spectra were recorded on a Nicolet 6500 spectrometer at a resolution of 4 cm⁻¹ in the range of 400–4000 cm⁻¹. Inherent viscosities (η_{inh}) of PAA were measured with an Ubbelohde viscometer at 25 °C in DMAc at a concentration of 0.5 g dL⁻¹. Dynamic mechanical analysis (DMA) was recorded on a TA instrument DMA Q800 at a heating rate of 5 °C min⁻¹ with a load frequency of 1 Hz in air, and *T_g* was regarded as the peak temperature of loss modulus (*E''*). Differential scanning calorimetric (DSC) analysis was carried out on a TA instrument DSC Q100 at a scanning rate of 10 °C min⁻¹ under nitrogen with 50 mL min⁻¹ gas flow. Thermo gravimetric analysis (TGA) was performed with a heating rate of 10 °C min⁻¹ under nitrogen atmosphere by the TA 2050. Thermo mechanical analysis (TMA) was conducted with a METTLER TMA/SDTA841 at a heating rate of 10 °C min⁻¹. The coefficient of thermal expansion (CTE) was recorded at the temperature range of 50–150 °C. The transmittance of the films was determined by Ultraviolet–visible (UV–vis) spectrometer (Shimadzu UV–Vis 2501). Mechanical properties were measured on a Shimadzu AG-I universal testing apparatus with crosshead speed of 5 mm min⁻¹, tensile modulus (*T_M*), tensile

strength (*T_S*) and elongation at break (*E_B*) were calculated as the average of five strips.

2.3. Synthesis of monomers

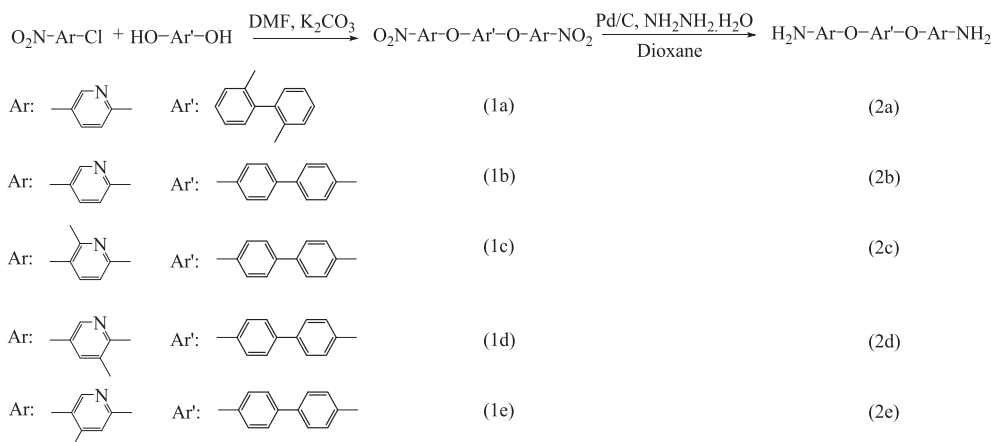
2.3.1. Synthesis of dinitro monomers (1a–e)

The synthesis of 2,2'-bis(5-nitro-2-pyridinoxy)biphenyl (1a) is used as an example to illustrate the detailed synthetic procedures. Under the protection of nitrogen, 2,2'-Dihydroxybiphenyl (5.59 g, 30 mmol), potassium carbonate (9.12 g, 66 mmol), and DMF (60 mL) were added into a dry round bottom flask with a stir bar. The mixture was allowed to stir at room temperature for 1 h. Next, 2-chloro-5-nitropyridine (10.46 g, 66 mmol) was added into the flask and the mixture was allowed to react at 80 °C for 7 h. Then, the obtained mixture was poured into 500 mL of distilled water. The crude product was collected by filtration, washed with water, and dried in vacuo at 80 °C for 10 h. After the crude product was recrystallized from DMF/water, 11.88 g of 1a was obtained (92%); Melting point: 141–143 °C (DSC). FT-IR (KBr): 1602, 1582, 1508, 1464, 1393, 1271, 1198, 1117 cm⁻¹; ¹H NMR (CDCl₃, ppm): 8.91 (d, 1H), 8.34 (dd, 1H), 7.40 (m, 2H), 7.20 (m, 2H), 6.80 (d, 1H); HRLC-MS (ESI): 431.3 (M + H)⁺, Calcd 430.4 for C₂₂H₁₄N₄O₆.

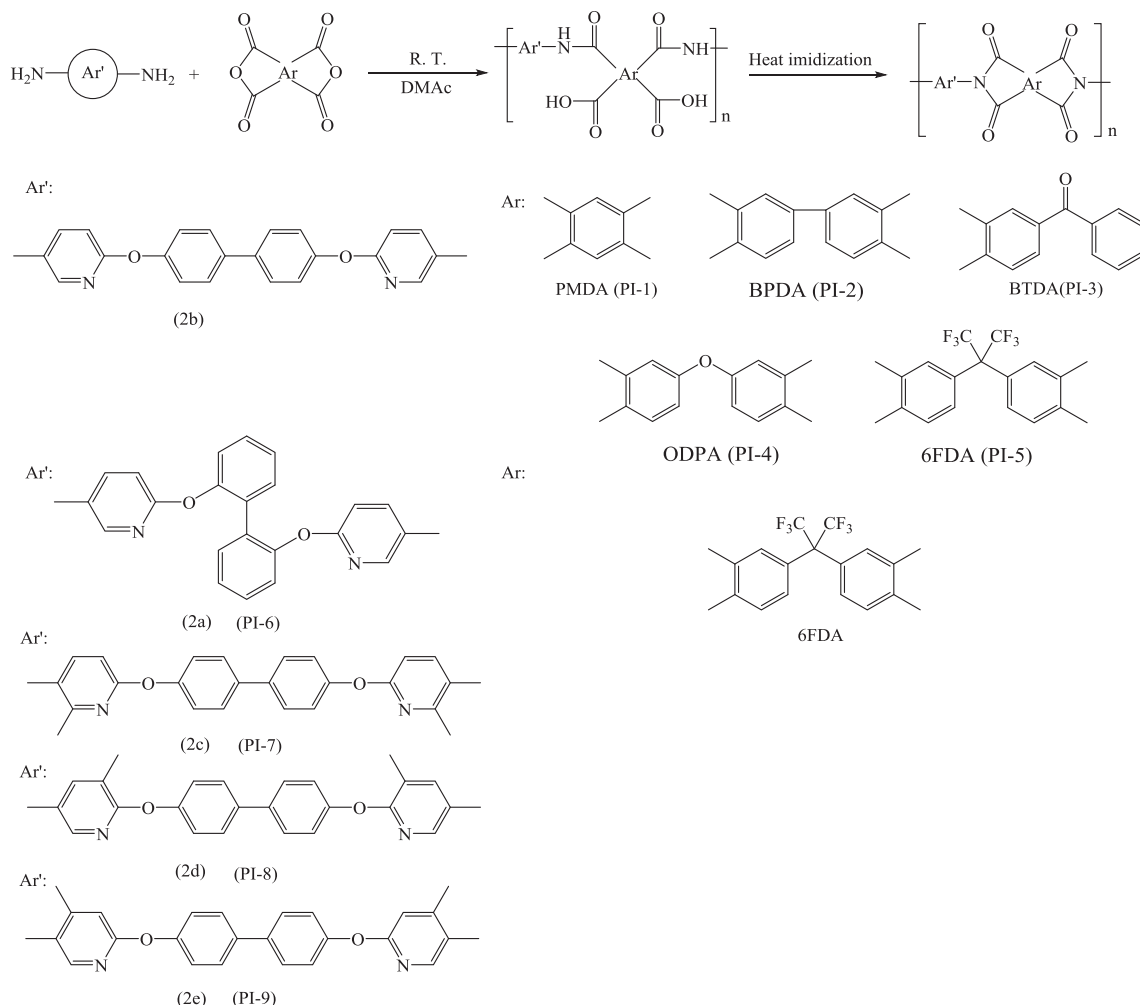
2.3.1.1. Synthesis of 4,4'-bis(5-nitro-2-pyridinoxy)biphenyl (1b). Recrystallized from DMF/water; Yield: 95%. Melting point: 197–198 °C (DSC). FT-IR (KBr): 1607, 1590, 1520, 1462, 1392, 1264, 1199, 1105 cm⁻¹; ¹H NMR (DMSO-d₆, ppm): 9.03 (d, 1H), 8.62 (dd, 1H), 7.80 (m, 2H), 7.30 (m, 2H), 7.27 (d, 1H); HRLC-MS (ESI): 431.3 (M + H)⁺, Calcd 430.4 for C₂₂H₁₄N₄O₆.

2.3.1.2. 4,4'-bis(5-nitro-6-methyl-2-pyridinoxy)biphenyl (1c). Recrystallized from DMF/water; Yield: 80%. Melting point: 185–187 °C (DSC). FT-IR (KBr): 1601, 1574, 1515, 1438, 1391, 1268, 1169, 1077 cm⁻¹; ¹H NMR (DMSO-d₆, ppm): 8.52 (d, 1H), 7.80 (d, 2H), 7.33 (d, 2H), 7.09 (d, 1H), 2.62 (s, 3H); HRLC-MS (ESI): 459.3 (M + H)⁺, Calcd 458.4 for C₂₄H₁₈N₄O₆.

2.3.1.3. 4,4'-bis(5-nitro-3-methyl-2-pyridinoxy)biphenyl (1d). Recrystallized from DMF/water; Yield: 82%. Melting point: 259–261 °C (DSC). FT-IR (KBr): 1586, 1516, 1455, 1383, 1258, 1202, 1106 cm⁻¹; ¹H NMR (DMSO-d₆, ppm): 8.87 (d, 1H), 8.59 (d, 1H), 7.78 (d, 2H), 7.33 (d, 2H), 2.50 (s, 1H); HRLC-MS (ESI): 459.2 (M + H)⁺, Calcd 458.4 for C₂₄H₁₈N₄O₆.



Scheme 1. Preparation of the monomers.



Scheme 2. Preparation of the polyimides (PIs).

2.3.1.4. 4,4'-bis(5-nitro-4-methyl-2-pyridinoxy)biphenyl (1e). Recrystallized from DMF/water; Yield: 75%. Melting point: 203–205 °C (DSC). FT-IR (KBr): 1597, 1510, 1468, 1390, 1255, 1202, 1099 cm^{-1} ; ^1H NMR (DMSO- d_6 , ppm): 8.87 (s, 1H), 7.78 (m, 2H), 7.30 (m, 2H), 7.26 (s, 2H), 2.62 (d, 3H); HRLC-MS (ESI): 459.3 ($\text{M} + \text{H}^+$), Calcd 458.4 for $\text{C}_{24}\text{H}_{18}\text{N}_4\text{O}_6$.

2.3.2. Synthesis of diamine monomers (2a–e)

The synthesis of 2,2'-bis(5-amino-2-pyridinoxy)biphenyl (2a) is used as an example to illustrate the detailed synthetic procedures. The dinitro compound (1a) (10.0 g, 23.2 mol), 10% Pd/C (0.9 g), and dioxane (100 mL) were added into a 250 mL flask with a stir bar. The suspension solution was heated to refluxing under nitrogen, and 80% hydrazine monohydrate (25 mL) was added dropwise to the mixture over 1 h. After a further 6 h of refluxing, the hot mixture was filtered to remove the catalyst, and the filtrate was distilled to remove some solvent. The obtained mixture was poured into 500 mL of stirring water to produce a solid precipitate which was filtered out, washed with water. After the crude product was recrystallized from dioxane/water, the precipitate was filtered and dried under vacuum at 80 °C overnight. Yield: 7.9 g (92%); Melting point: 179–181 °C (DSC). FT-IR (KBr): 3456, 3359, 1617, 1577, 1541, 1485, 1233, 1164, 1118 cm^{-1} ; ^1H NMR (DMSO- d_6 , ppm): 7.51 (d, 1H), 7.31 (m, 2H), 7.10 (dd, 2H), 6.90 (dd, 1H), 6.60 (d, 1H), 5.21 (s, 2H); ^{13}C NMR (DMSO- d_6 , ppm): 154.2, 153.2, 140.8, 132.4, 128.4, 125.4,

122.5, 119.7, 112.3; HRLC-MS (ESI): 371.3 ($\text{M} + \text{H}^+$), Calcd 370.4 for $\text{C}_{22}\text{H}_{18}\text{N}_4\text{O}_2$. Elemental analysis: Calculated for $\text{C}_{22}\text{H}_{18}\text{N}_4\text{O}_2$: C, 71.34%, H, 4.90%, N, 15.13%; Found: C, 71.18%, H, 4.96%, N, 15.02%.

2.3.2.1. 4,4'-bis(5-amino-2-pyridinoxy)biphenyl (2b).

Recrystallized from dioxane/water; Yield: 84%. Melting point: 216–218 °C (DSC). FT-IR (KBr): 3413, 3358, 1631, 1584, 1477, 1241, 1150, 1105 cm^{-1} ; ^1H NMR (DMSO- d_6 , ppm): 7.60 (m, 1H), 7.57 (dd, 2H), 7.12 (m, 1H), 7.02 (m, 2H), 6.80 (m, 1H), 5.13 (s, 2H); ^{13}C NMR (DMSO- d_6 , ppm): 155.6, 153.4, 142.0, 134.4, 132.3, 127.5, 125.3, 118.8, 112.9; HRLC-MS (ESI): 371.3 ($\text{M} + \text{H}^+$), Calcd 370.4 for $\text{C}_{22}\text{H}_{18}\text{N}_4\text{O}_2$. Elemental analysis: Calculated for $\text{C}_{22}\text{H}_{18}\text{N}_4\text{O}_2$: C, 71.34%, H, 4.90%, N, 15.13%; Found: C, 71.12%, H, 4.98%, N, 15.02%.

2.3.2.2. 4,4'-bis(5-amino-6-methyl-2-pyridinoxy)biphenyl (2c).

Recrystallized from dioxane/water; Yield: 86%. Melting point: 219–221 °C (DSC). FT-IR (KBr): 3380, 3222, 1635, 1598, 1494, 1252, 1167 cm^{-1} ; ^1H NMR (DMSO- d_6 , ppm): 7.60 (m, 2H), 7.08 (d, 1H), 6.99 (t, 2H), 6.67 (d, 1H), 4.90 (s, 2H), 2.19 (s, 3H); ^{13}C NMR (DMSO- d_6 , ppm): 155.3, 152.0, 139.7, 134.3, 127.4, 124.8, 118.6, 110.8, 88.6, 20.1; HRLC-MS (ESI): 399.3 ($\text{M} + \text{H}^+$), Calcd 398.5 for $\text{C}_{22}\text{H}_{18}\text{N}_4\text{O}_2$. Elemental analysis: Calculated for $\text{C}_{24}\text{H}_{22}\text{N}_4\text{O}_2$: C, 72.34%, H, 5.57%, N, 14.06%; Found: C, 72.16%, H, 5.76%, N, 13.98%.

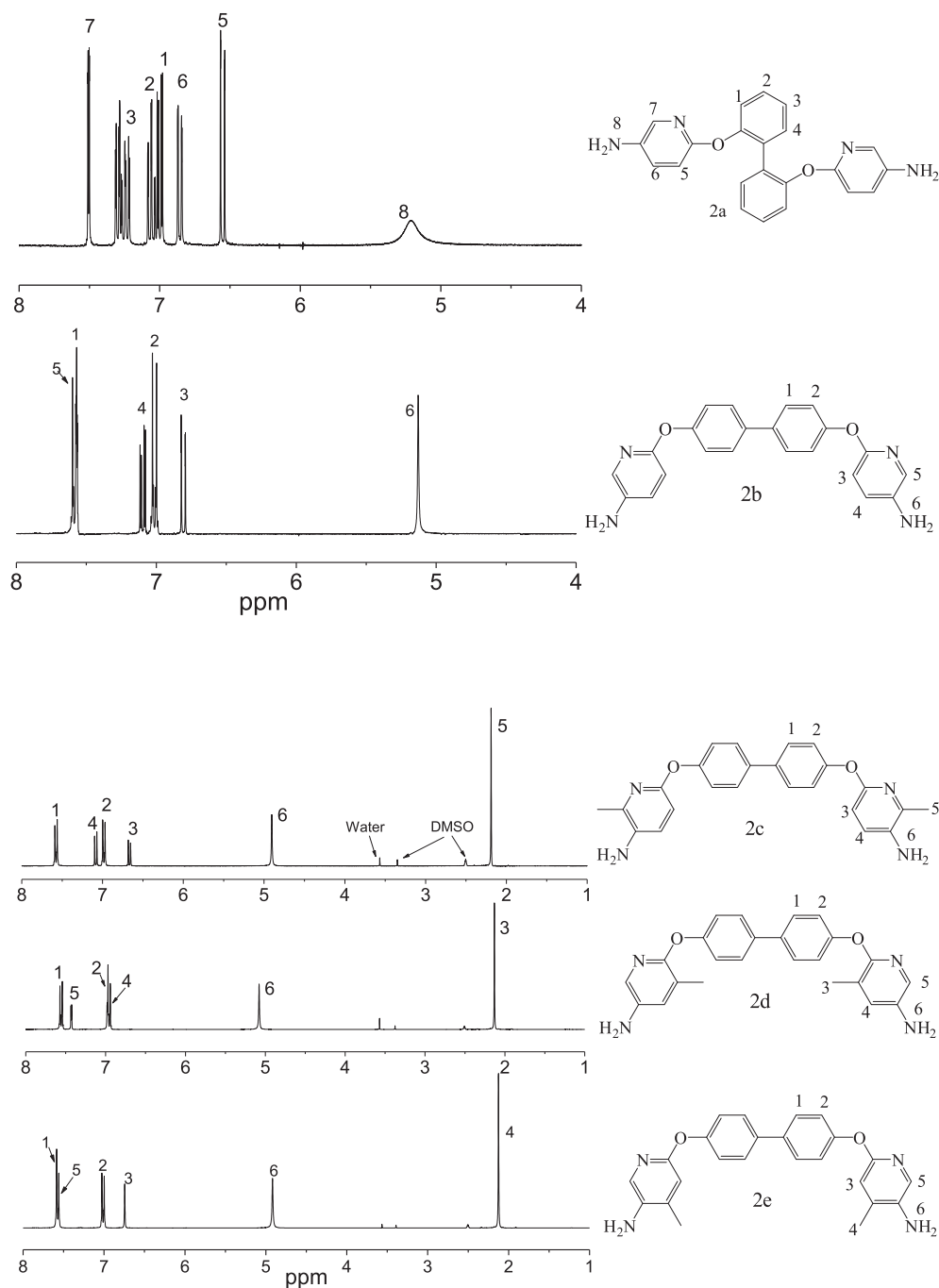


Fig. 1. ^1H NMR spectra of diamines 2a–e.

2.3.2.3. 4,4'-bis(5-amino-3-methyl-2-pyridinoxy)biphenyl (2d). Recrystallized from dioxane/water; Yield: 92%. Melting point: 180–182 °C (DSC). FT-IR (KBr): 3418, 3329, 1604, 1493, 1472, 1232, 1165 cm^{-1} ; ^1H NMR (DMSO- d_6 , ppm): 7.56 (m, 2H), 7.43 (d, 1H), 6.98 (t, 2H), 6.93 (m, 1H), 5.08 (s, 2H), 2.16 (d, 3H); ^{13}C NMR (DMSO- d_6 , ppm): 155.8, 151.4, 142.4, 134.1, 130.0, 127.4, 125.8, 122.5, 118.6, 15.6; HRLC-MS (ESI): 399.3 ($\text{M} + \text{H}^+$), Calcd 398.5 for $\text{C}_{22}\text{H}_{18}\text{N}_4\text{O}_2$. Elemental analysis: Calculated for $\text{C}_{24}\text{H}_{22}\text{N}_4\text{O}_2$: C, 72.34%, H, 5.57%, N, 14.06%; Found: C, 72.12%, H, 5.74%, N, 13.96%.

2.3.2.4. 4,4'-bis(5-amino-4-methyl-2-pyridinoxy)biphenyl (2e). Recrystallized from dioxane/water; Yield: 90%. Melting point:

204–206 °C (DSC). FT-IR (KBr): 3415, 3303, 1640, 1606, 1487, 1235, 1164, 1140 cm^{-1} ; ^1H NMR (DMSO- d_6 , ppm): 7.59 (d, 2H), 7.56 (s, 1H), 7.01 (d, 2H), 6.74 (s, 1H), 4.92 (s, 2H), 2.15 (d, 3H); ^{13}C NMR (DMSO- d_6 , ppm): 155.6, 153.8, 140.6, 134.8, 134.4, 131.9, 127.4, 119.2, 113.4, 17.0; HRLC-MS (ESI): 399.3 ($\text{M} + \text{H}^+$), Calcd 398.5 for $\text{C}_{22}\text{H}_{18}\text{N}_4\text{O}_2$. Elemental analysis: Calculated for $\text{C}_{24}\text{H}_{22}\text{N}_4\text{O}_2$: C, 72.34%, H, 5.57%, N, 14.06%; Found: C, 72.20%, H, 5.70%, N, 13.94%.

2.4. Synthesis of polyimides

The polyimides were synthesized by the conventional two-step procedure via poly(amic acid) precursors, followed by thermally

Table 1
Characteristics of the polyimides.

Polyimides	η_{inh} of PAA (dL g ⁻¹) ^a	Composition of repeating unit	Elemental analysis (%)			
				C	H	N
PI-1	0.98	C ₃₂ H ₁₆ N ₄ O ₆	Calacd	69.57	2.92	10.14
			Found	69.05	3.12	9.90
PI-2	0.85	C ₃₈ H ₂₀ N ₄ O ₆	Calacd	72.61	3.21	8.91
			Found	72.44	3.29	8.66
PI-3	1.18	C ₃₉ H ₂₀ N ₄ O ₇	Calacd	71.29	3.14	8.53
			Found	71.09	3.22	8.40
PI-4	1.58	C ₃₈ H ₂₀ N ₄ O ₇	Calacd	70.81	3.13	8.69
			Found	70.51	3.28	8.52
PI-5	1.66	C ₄₁ H ₂₀ F ₆ N ₄ O ₆	Calacd	63.25	2.59	7.20
			Found	63.27	2.68	7.01
PI-6	1.49	C ₄₁ H ₂₀ F ₆ N ₄ O ₆	Calacd	63.25	2.59	7.20
			Found	63.17	2.70	6.99
PI-7	1.26	C ₄₃ H ₂₄ F ₆ N ₄ O ₆	Calacd	64.02	3.00	6.95
			Found	63.95	3.10	6.89
PI-8	1.19	C ₄₃ H ₂₄ F ₆ N ₄ O ₆	Calacd	64.02	3.00	6.95
			Found	63.93	3.12	6.87
PI-9	1.33	C ₄₃ H ₂₄ F ₆ N ₄ O ₆	Calacd	64.02	3.00	6.95
			Found	63.93	3.14	6.85

^a Inherent viscosities of PAA was measured at 25 °C with a concentration of 0.5 g dL⁻¹ in DMAc.

curing at elevated temperatures. Only the polymerization of polyimide **PI-1 (PMDA/2b)** is described as an example. To a solution of 1.4816 g (4.0 mmol) of diamine **2b** in 7.06 g DMAc, 0.8725 g (4.0 mmol) of PMDA was added in one portion. Extra 6.28 g DMAc was added to adjust the solid content 15 wt %. The solution was stirred at room temperature under nitrogen for 2–12 h to yield a viscous poly (amic acid) (PAA) solution, followed by thermal imidization at elevated temperatures (as shown in [Scheme 2](#)). PI films were prepared by thermal imidization of PAA solutions cast onto glass plates, followed by a preheating program (80 °C/3 h, 120 °C/0.5 h, 150 °C/0.5 h) and an imidization procedure under vacuum (200 °C/0.5 h, 250 °C/0.5 h, 300 °C/1 h). The freestanding films were obtained by soaking in water to release from the glass substrates.

PI-2(BPDA/2b), **PI-3(BTDA/2b)**, **PI-4(ODPA/2b)**, **PI-5(6FDA/2b)**, **PI-6(6FDA/2a)**, **PI-7(6FDA/2c)**, **PI-8(6FDA/2d)** and **PI-9(6FDA/2e)** were synthesized by the similar method described above.

3. Results and discussion

3.1. Monomer synthesis

Two series of novel isomeric aromatic diamines, **2a**, **2b** and **2c**, **2d**, **2e** were designed to provide systematic variations in chemical structure presented in [Scheme 1](#). The S_NAr reactions was used to prepare the intermediate dinitro compounds (**1a–e**) which were reduced to the desired containing pyridine and biphenyl diamines (**2a–e**) using hydrazine catalyzed by Pd/C.

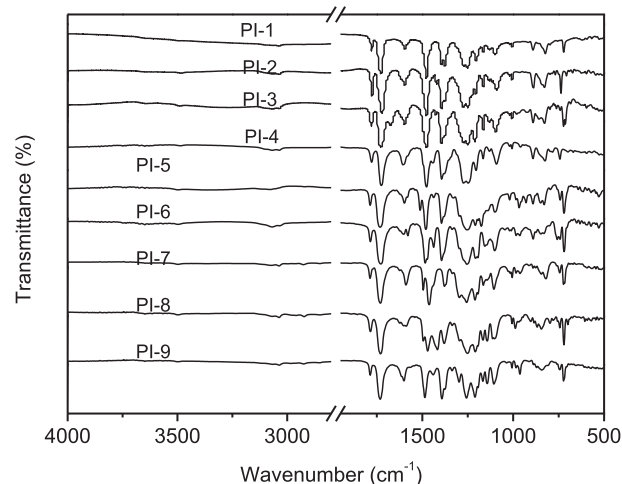
The structures of diamines (**2a–e**) were confirmed by elemental analysis, HPLC-MS, FT-IR spectra, and ¹H NMR and ¹³C NMR spectroscopy. As shown in [Fig. 1](#), ¹H NMR spectrum of the diamine monomers (**2a–e**) illustrate that the nitro groups in **1a–e** were completely reduced, in which the signal of amino groups appeared at around δ 5.0 as a singlet. All the spectroscopic data obtained agreed with the expected structures.

3.2. Polymer synthesis

The diamine monomers, **2a–e** were reacted with commercially available aromatic dianhydrides to give two series of new polyimides, PI-(1–5) and PI-(5–9), respectively, as shown in [Scheme 2](#). The new polyimides were synthesized using two-step methods,

which were carried out via poly(amic acid)s (PAA) intermediate. The polymerization was carried out by reacting equimolar amounts of diamine monomer with aromatic dianhydrides at a concentration of 15% solids in DMAc. The polycondensation reaction was prepared at room temperature for 2–12 h yielded PAA solution. As shown in [Table 1](#), the inherent viscosities of the PAA precursors were 0.85–1.66 dL g⁻¹. Tough and flexible polyimide films were obtained by casting the PAA solution on glass plate followed by thermally curing process at 300 °C.

The chemical structures of polyimides were characterized by FT-IR, ¹H NMR and element analysis. [Fig. 2](#) demonstrates IR spectra for polyimide films. All the polyimides exhibited characteristic imide group absorptions around 1785 cm⁻¹ (asymmetrical C=O stretching), 1728 cm⁻¹ (symmetrical C=O stretching), 1394 cm⁻¹ (C–N stretching), and together with some strong absorption bands in the region of 1300–1100 cm⁻¹ (C–O and C–F stretching). There was no existence of the characteristic absorption bonds of the amide group near 3220–3450 cm⁻¹ (N–H stretching) and 1580–1620 cm⁻¹ (N–H bend), which indicated polymers had been fully imidized. [Fig. 3](#) depicts two typical ¹H NMR spectrum of the aromatic polyimide **PI-5** and **PI-6**, in which all the protons in the polymer

**Fig. 2.** FT-IR spectra of the polyimides.

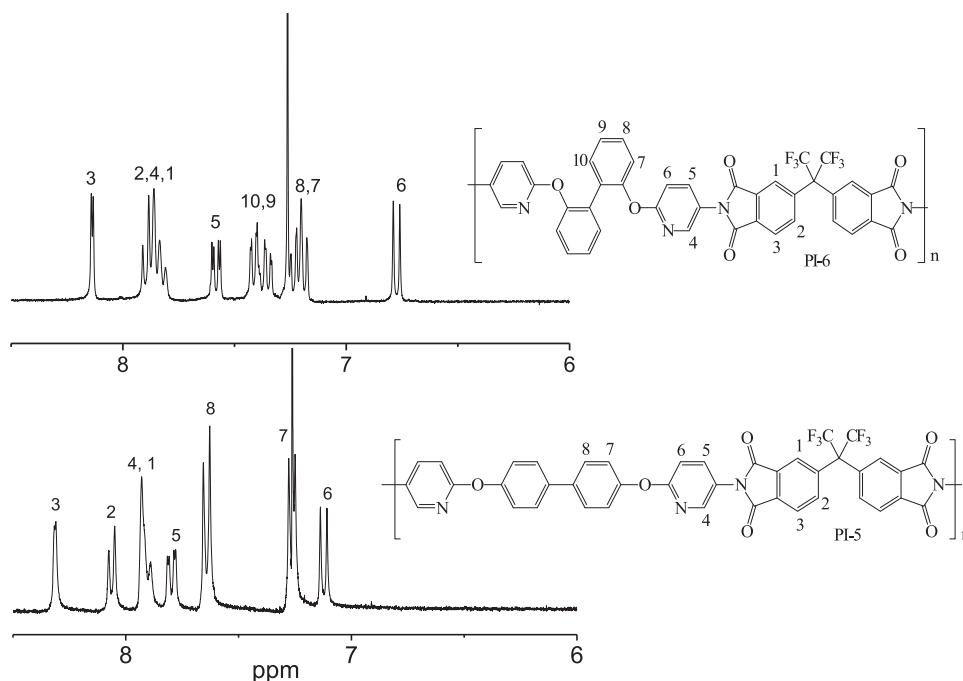


Fig. 3. ^1H NMR spectra of PI-5 and PI-6.

backbone can be assigned. The results of the elemental analyses of all the thermally cured polyimides were listed in Table 1. The values found were in good agreement with the calculated ones of the proposed structures.

3.3. Morphologies of polyimides

The morphological structure of the PI films was analyzed by Wide-Angle X-ray Diffraction (WAXD), 2θ ranging from 0 to 50° , using the polyimide films and the results were shown in Fig. 4. PI-2 (BPDA/2b) exhibits a fair degree of crystallinity, which might be attributed to the rigid structure and regular arrangements [15] of BPDA and 4,4'-biphenylene. However the other polyimides express a set of wider diffraction peak and these should be evidences that indicate the polyimides holding morphology, which is attributed to the incorporation of flexible ether linkage and methyl substituted pyridine loosening the chain packing of the polymer and the

pyridyl ether linkage units having the twist polymer backbone structure [25].

3.4. Thermal properties of polyimides

The thermal properties of the polyimides, PI-(1–9) were evaluated by differential scanning calorimetry (DSC), dynamic mechanical analysis (DMA), thermo gravimetric analysis (TGA) and thermo mechanical analysis (TMA). The results are summarized in Table 2. Glass transition temperatures (T_g) of the polyimides were in the range of $249\text{--}313^\circ\text{C}$ and $241\text{--}348^\circ\text{C}$, as obtained by DSC (Fig. 5) and DMA (Fig. 6), respectively. The slight differences of T_g

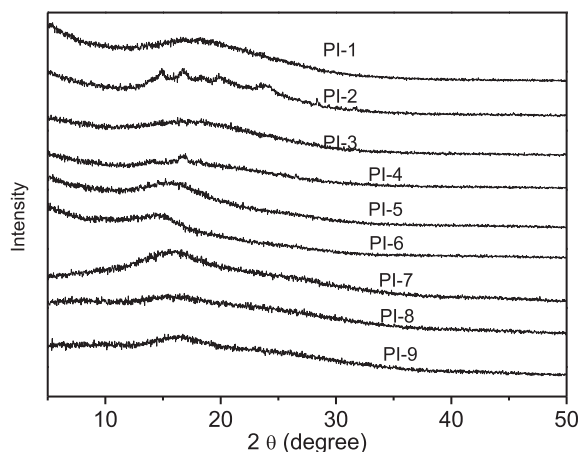


Fig. 4. Wide-angle X-ray diffraction patterns of PI films.

Table 2
Thermal properties of the PI films.

Polyimides	T_g ($^\circ\text{C}$)		Td ($^\circ\text{C}$) ^c	T5% ($^\circ\text{C}$) ^d	T10% ($^\circ\text{C}$) ^d	Rw (%) ^e	CTE ($\text{ppm}^\circ\text{C}^{-1}$) ^f
	DSC ^a	DMA ^b					
PI-1	309	348	525	530	551	61.8	21
PI-2	266	262	523	533	558	65.1	38
PI-3	283	261	512	514	541	61.5	25
PI-4	276	253	491	509	529	60.8	52
PI-5	303	290	516	523	543	58.7	51
PI-6	249	241	503	507	527	59.9	62
PI-7	309	293	462	471	494	61.1	60
PI-8	299	285	493	484	519	56.9	62
PI-9	313	305	495	489	519	59.4	61

^a Obtained at the baseline shift in the second heating DSC traces, with a heating rate of $10^\circ\text{C min}^{-1}$ under N_2 .

^b Measured by DMA at a heating rate of 5°C min^{-1} and a load frequency of 1 Hz in film tension geometry.

^c Onset decomposition temperature by TGA at a heating rate of $10^\circ\text{C min}^{-1}$ under N_2 .

^d 5% and 10% weight loss temperatures measured by TGA at a heating rate of $10^\circ\text{C min}^{-1}$ under N_2 .

^e Residual weight retention at 800°C by TGA at a heating rate of $10^\circ\text{C min}^{-1}$ under N_2 .

^f CTE, coefficient of thermal expansion is recorded from 50 to 150°C at a heating rate of $10^\circ\text{C min}^{-1}$ by TMA.

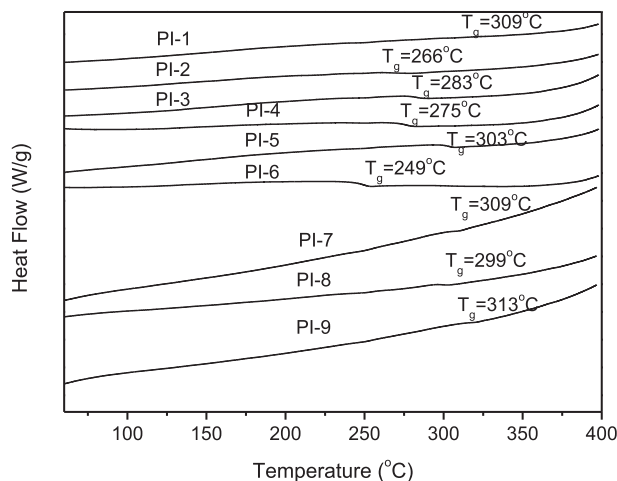


Fig. 5. DSC curves of PI films.

values obtained by DSC and DMA were mainly attributed to the different responses of the samples to the two characterization methods. Generally, T_g values of polymers are determined by molecular packing and chain rigidity of the polymer backbones. As a result, in PI-(1–6) the polyimides PI-1 derived from PMDA and 2b with the most rigid polymer backbone exhibited the highest T_g . PI-5 (derived from 6FDA and 2b) showing a higher T_g value than that of PI-3 (derived from BTDA and 2b). This might be attributed to

inhibition of free rotation of the polymer segments due to the existence of CF_3 group in the backbone [26]. The T_g (303 °C) of PI-5 derived from 6FDA and 2b, was 54 °C higher than that (249 °C) of isomeric PI-6 derived from 6FDA and 2a, which was attributed to the distorted 2a monomer structure incorporated into polymer structure of PI-6 lowering the T_g . In PI-(7–9), as seen from Fig. 5, the corresponding T_g sequence is PI-9(313 °C) > PI-7(309 °C) > PI-8(299 °C). The PI-9 and PI-7 exhibited the higher T_g than that of PI-8 which may be due to the *ortho*-methyl-substituted amino inhibiting rotation of the imide ring to improve the T_g . However, PI-8 showed the lower T_g than PI-5 which may be attributed to *meta*-methyl-substituted amino loosening molecular packing.

Fig. 7 shows the TMA curves of the polyimide films. The coefficients of thermal expansion (CTEs) of the polyimides ranged from 21 to 62 $\text{ppm } ^\circ\text{C}^{-1}$ (Table 2). CTEs are associated with the rigidity and linearity of the polymer chain, which affects the chain packing. PI-1 (PMDA/2b) exhibited the lowest CTEs due to its highest rigidity and linearity of the polymer chain, and PI-6 (6FDA/2a) exhibited the higher CTEs which were probably attributed to the flexible and twisted chain structure. PI-7(6FDA/2c), PI-8(6FDA/2d) and PI-9(6FDA/2e) showed the similar CTEs with PI-6 (6FDA/2a) which may be explained by the similar linearity of polymer chain.

Fig. 8 shows the TGA curves of the polyimide films. The TGA of the PIs were evaluated at a heating rate of $10 ^\circ\text{C min}^{-1}$ in nitrogen and the results are summarized in Table 2. As can be seen from Fig. 8(a), the polyimides PI-(1–6) did not show obvious weight loss before 490 °C, implying that no thermal decomposition occurred. 5% and 10% weight loss temperatures ($T_5\%$ and $T_{10}\%$) were located

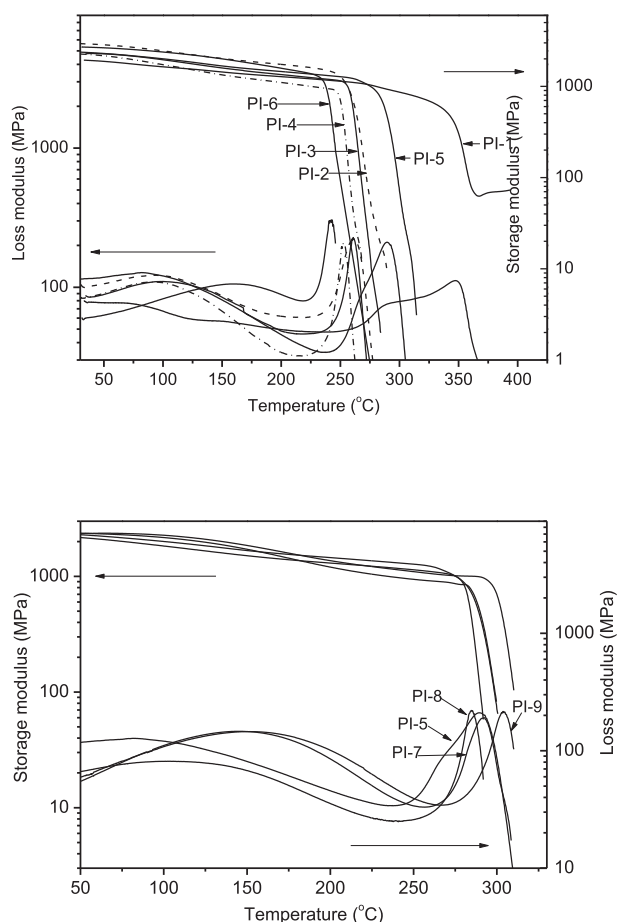


Fig. 6. Loss and storage modulus of polyimide films in DMA.

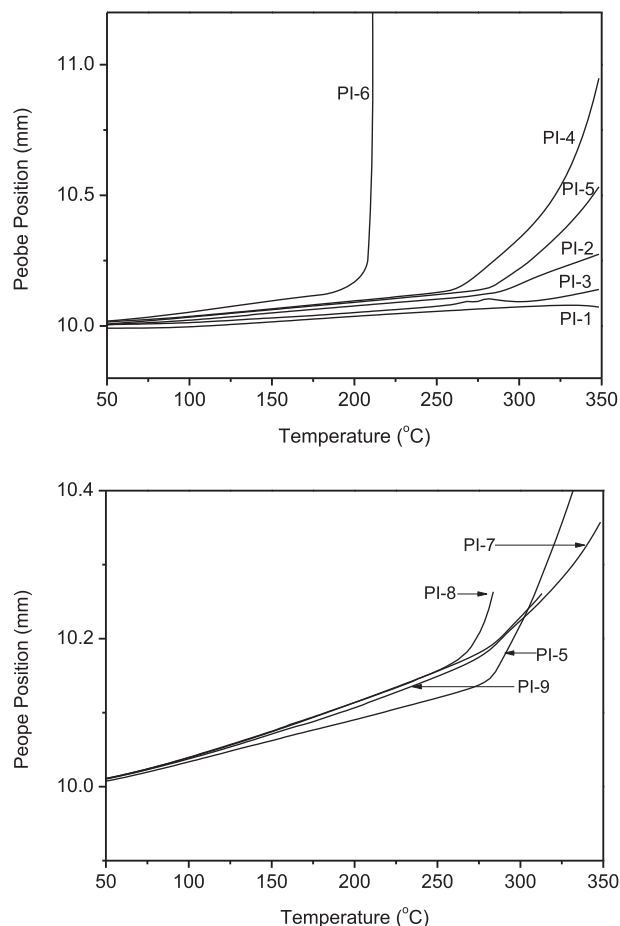


Fig. 7. TMA curves of the polyimide films.

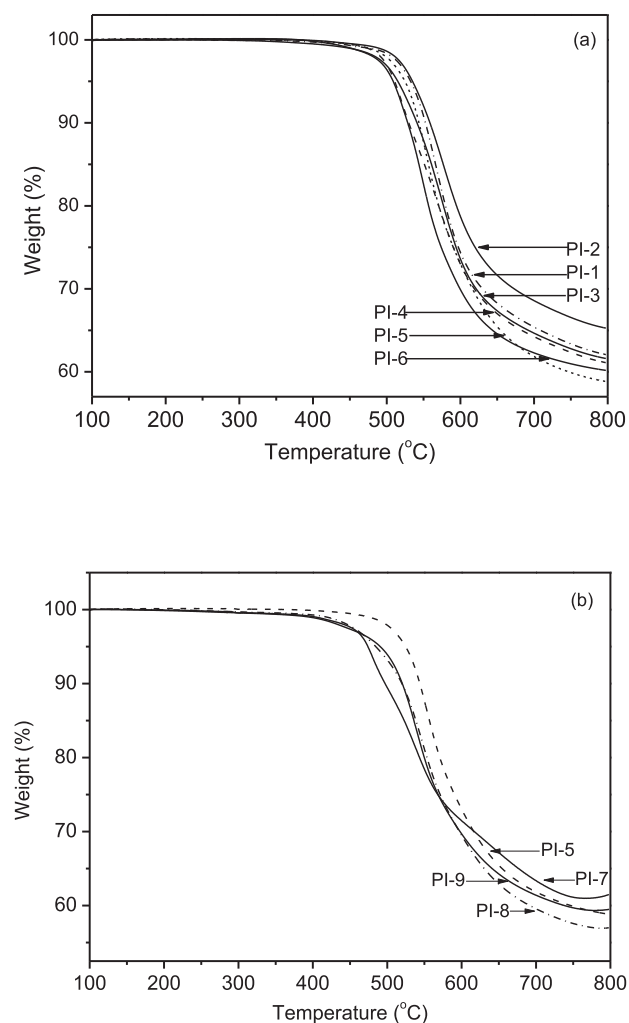


Fig. 8. TGA curves of PI films in nitrogen.

in the range of 507–533 °C and 527–558 °C in nitrogen, respectively. The residual weight retentions at 800 °C were in the range of 58.7–65.1% in nitrogen. PI-2 derived from BPDA and 2b exhibited the highest char yield 65.1% at 800 °C under the atmosphere of nitrogen by comparison with other polyimides, which might be attributed to the presence of higher char content in the polymer backbone. As can be seen from Fig. 8(b), 5% and 10% weight loss temperatures (T5% and T10%) of the polyimides PI-(7–9) were

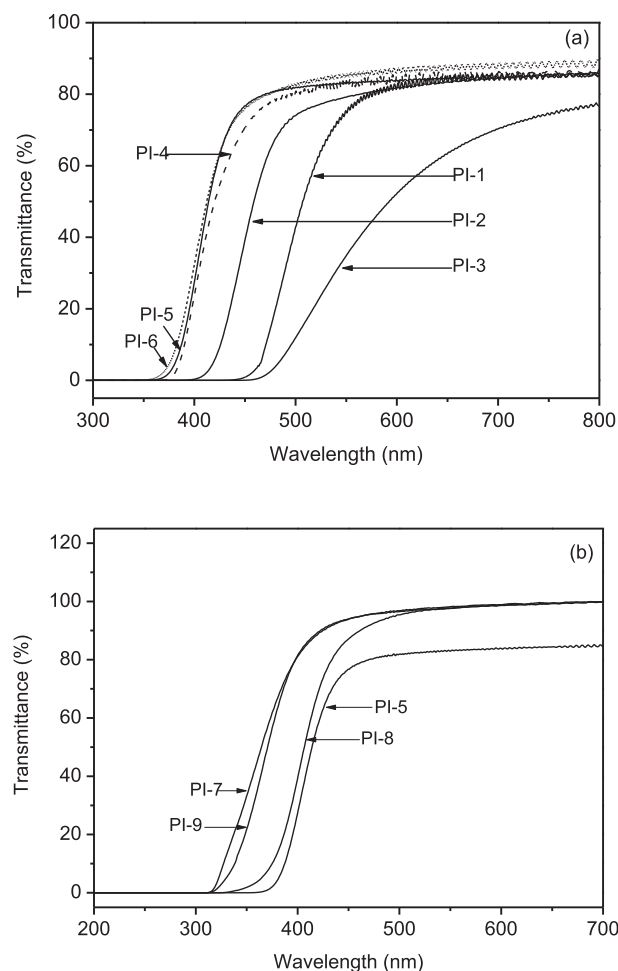


Fig. 9. UV-vis spectra of the polyimide films.

located in the range of 471–489 °C and 494–519 °C in nitrogen, respectively, and the residual weight retentions at 800 °C were in the range of 59.4–61.1% in nitrogen. The corresponding Td and T5% sequence was PI-9 > PI-8 > PI-7. The results showed the thermal stability of PI-(7–9) was *para*-methyl-substituted pyridyl PI > *meta*-methyl-substituted pyridyl PI > *ortho*-methyl-substituted pyridyl PI, when the anhydride was fixed. Meanwhile, the Td, T5% and T10% of methyl-substituted polyimide PI-(7–9) were lower than that of non-methyl-substituted polyimide PI-(5). TGA results indicated that the obtained polyimides possessed fairly good thermal stability. Meanwhile, the TGA results of the polyimides also indicated that the pyridine unit incorporated into the polymer backbone did not deteriorated the thermal property. The onset decomposition temperature (Td) of PI-6 was higher than that of ref-PI-1 and ref-PI-2 which indicated the pyridine ring incorporated into polymer backbone gave a benefit to improve the onset decomposition temperature.

3.5. Mechanical properties of the polyimides

The polyimide films were tested for mechanical properties at room temperature, as summarized in Table 3. The polyimide films had the tensile strength as high as 134 MPa, the tensile modulus in range of 2.1–3.6 GPa, and the elongation at break of 5.4–21.3%, indicating that the obtained polyimide films were tough and strong. In comparison of the mechanical property of PI-5 (6FDA/2b) and PI-6 (6FDA/2a), the former exhibited the higher tensile

Table 3
Mechanical, optical properties and water uptake of PI films.

Polyimides	T_S^a (MPa)	T_M^b (GPa)	E_B^c (%)	$\lambda_{cut-off}$ (nm)
PI-1	105 ± 2.4 ^d	2.1 ± 0.22	17.6 ± 0.6	437
PI-2	106 ± 1.8	2.1 ± 0.20	16.1 ± 0.8	394
PI-3	128 ± 3.5	3.5 ± 0.28	21.3 ± 1.0	455
PI-4	102 ± 2.2	2.8 ± 0.30	20.9 ± 1.0	371
PI-5	122 ± 2.9	3.2 ± 0.29	8.2 ± 0.8	359
PI-6	103 ± 2.6	3.1 ± 0.26	5.4 ± 0.6	351
PI-7	134 ± 3.4	3.1 ± 0.30	4.2 ± 1.2	310
PI-8	108 ± 2.8	3.2 ± 0.20	6.1 ± 1.0	328
PI-9	130 ± 3.0	3.6 ± 0.28	4.4 ± 1.4	311

^a T_S , Tensile strength.

^b T_M , Tensile modulus.

^c E_B , Elongation at break.

^d 2.4, standard deviation.

strength, tensile modulus and elongation at break than the latter. It might be attributed to the bent and distorted structure of polyimide backbone derived from 2a. The PI-7 and PI-9 showed the very high tensile strength 134 and 130 MPa which may be explained by the *ortho*-methyl-substituted amino inhibiting rotation of the imide ring to improve the rigidity of polyimide backbone.

3.6. Optical properties of polyimides

The optical transparency of polyimide films with thicknesses of approximately 10 μm were measured by UV–vis spectroscopy, and the value of cut-off wavelength ($\lambda_{\text{cut-off}}$) was used as the parameter to evaluate transparency. As listed in Table 3, $\lambda_{\text{cut-off}}$ values were in the range of 310–455 nm. Fig. 9 shows UV–Vis absorption spectra of the polyimides. 6FDA and ODPa produce fairly transparent PI films in contrast to other dianhydrides. On the other hand, polyimides based on PMDA, BPDA and BTDA have low transparency in the UV-visible region. When the diamine structures are fixed, the cut-off wavelengths of PI films are directly related to the color intensity of polyimide films and the electron withdrawing properties of the dianhydrides. S. Ando [27] reported the arrangements of dianhydrides in the order of color intensity of polyimides from deep to pale when the diamine structures were fixed: BTDA > PMDA > BPDA > ODPa > 6FDA. As seen from Fig. 9(a), PI-5 (6FDA/2b) exhibits higher transparency and lower $\lambda_{\text{cut-off}}$ value than that of PI-4 (ODPa/2b). PI-6 (6FDA/2a) exhibits the lower $\lambda_{\text{cut-off}}$ value than that of PI-5 (6FDA/2a) which may be explained by the distorted structure of PI-6 reducing the formation CTCs [28]. The light colors of polyimides derived from 6FDA having $-\text{C}(\text{CF}_3)_2-$ groups in their dianhydride moieties can be explained from the decreased intermolecular interactions. As seen from Fig. 9(b), the $\lambda_{\text{cut-off}}$ values of the PI films were 310 nm (PI-7) \leq 311 nm (PI-9) < 328 nm (PI-8). This is attributable to the *ortho* methyl groups in the aromatic diamines, which induce significant steric hindrance around the C–N imide bond and the significantly distorted conformations in PI-7 and PI-9 effectively reduce the formation of intramolecular and intermolecular CTCs in the main chains [28]. Transmittance (%) of the polyimide films at 400 nm decreased in the order of 82% (PI-9) > 81% (PI-7) > 39% (PI-8).

3.7. Solubility of polyimides

Solubility of the polyimides was determined at room temperature for 24 h and the results were summarized in Table 4. In PI-(1–6), PI-4, PI-5 and PI-6 showed better solubility than other polymers, due to their distinguishing backbone structures: PI-6 derived from 6FDA and 2a possessed bent and distorted polymer

chain conformation arising from the dianhydride and diamine component, the intermolecular interaction of PI-6 was weak, enduing PI-6 with better solubility [29,30], bulky pendant CF_3 group of 6FDA derived PI-5 inhibited close packing of the polymer chain¹⁵, making PI-5 easier to be dissolved; flexible ether linkage of ODPa component also imparted PI-4 better solubility. PI-6 (6FDA/2a) has better solubility than the comparable PI-5 (6FDA/2b) in polar and non-polar solvents which is attributed to the bent and distorted chain structure. This improvement in the organo-solubility of the PI-4 derived from ODPa and 2b can be partly attributed to the incorporation of nitrogen-containing pyridine ring into PI main chains, which disrupt the close packing of the polymer chains and decrease the intermolecular interactions. In PI-(7–9), PI-8 (6FDA/2d) showed the better solubility than PI-7 (6FDA/2c) and PI-9(6FDA/2e) which may be attributed to *meta*-methyl-substituted amino loosening molecular packing to improve the solubility.

4. Conclusions

Two series of novel isomeric aromatic containing pyridine and biphenyl unit diamines, 2,2'-bis(5-amino-2-pyridinoxy)biphenyl (2a), 4,4'-bis(5-amino-2-pyridinoxy)biphenyl (2b), and 4,4'-bis(5-amino-6-methyl-2-pyridinoxy)biphenyl (2c), 4,4'-bis(5-amino-3-methyl-2-pyridinoxy)biphenyl (2d), 4,4'-bis(5-amino-4-methyl-2-pyridinoxy)biphenyl (2e) were synthesized and characterized, which were employed to react with various aromatic dianhydrides to yield two series of novel polyimides through a typical two-step polymerization method. The experimental results show that the incorporation of methyl groups at the *ortho*-position of pyridine diamines is an effective way to improve the glass transition temperature, mechanical properties, solubility and optical transparency of PIs. These high optical transparency, high mechanical properties, and high thermal stability factors make the resulting PIs promising candidates for advanced optical device applications. In addition, through clarifying the structure-property relationship of the obtained polyimides, it is a great benefit to design novel structure monomers using pyridine and biphenyl groups for improving exceptional property.

Acknowledgments

Financial support from the National Nature Science Foundation of China (National 973 program No.G2010CB631100) and the National Technology Support Program (NO. 2011BAA06B03) are gratefully acknowledged.

References

- [1] Sroog CE. History of the invention and development of the polyimides. In: Ghosh MK, Mittal KL, editors. Polyimides fundamentals and applications. New York: Marcel Dekker; 1996. p. 1–6.
- [2] Mittal KL. Polyimides and other high-temperature polymers. Leiden, The Netherlands: VSP/Brill; 2009.
- [3] Bessonov MI, Koton MM, Kudryavtsev VV, Laius LA, editors. Polyimides. New York: Consultants Bureau; 1987.
- [4] Ghosh MK, Mittal KL, editors. Polyimides. New York: Marcel Dekker; 1996.
- [5] Takekoshi T. In: Kirk, editor. Encyclopedia of chemical technology, Vol. 19. New York: Wiley; 1996. p. 813–37.
- [6] Abadie MJ. High performance polymers-polyimides based-from chemistry to applications. In: Périchaud AA, Isakov RM, editors. Croatia; 2012. p. 215–44 [chapter 11].
- [7] Takeichi T, Tanikawa M. Microelectronics technology. 1995. p. 439–48 [Chapter 29].
- [8] Naskar AK, Edie DD. J Compos Mater 2006;40:1871–83.
- [9] Ma XH, Swaidan R. Macromolecules 2012;45:3841–9.
- [10] Lin SH, Li FM, Cheng SZ, Harris FW. Macromolecules 1998;31:2080–6.
- [11] You NH, Suzuki Y, Yorifuji D, Ando S, Ueda M. Macromolecules 2008;41: 6361–6.

Table 4
Solubility behavior of the polyimides^a.

Solvents	PI-1	PI-2	PI-3	PI-4	PI-5	PI-6	PI-7	PI-8	PI-9
<i>m</i> -Cresol	–	–	–	–	–	++	–	–	–
DMF	–	–	–	++	++	++	++	++	++
DMAc	–	–	–	++	++	++	++	++	++
NMP	–	–	–	++	++	++	++	++	++
DMSO	–	–	–	–	–	++	–	++	–
THF	–	–	–	–	–	++	–	++	–
Chloroform	–	–	–	–	++	++	++	++	++
Cyclohexanone	–	–	–	–	–	++	–	–	–
CH ₃ COOH	–	–	–	–	–	–	–	–	–
Pyridine	–	–	–	–	++	++	++	++	++

DMF = *N,N*-dimethylformamide; DMAc = *N,N*-dimethylacetamide; NMP = *N*-methyl-2-pyrrolidone; DMSO = Dimethyl sulfoxide; THF = Tetrahydrofuran.

++, soluble at room temperature; ++, partial soluble; –, insoluble.

^a Solubility was determined with 10 mg of polyimides in 1 mL of solvent at room temperature for 24 h.

- [12] Guo XX, Fang JH, Tanaka K, Kita H, Okamoto KI. *J Polym Sci Part A Polym Chem* 2004;42:1432–40.
- [13] Wang KL, Liu YL, Lee JW, Neoh KG, Kang ET. *Macromolecules* 2010;43:7159–64.
- [14] Li GY, Wang ZG. *Macromolecules* 2013;46:3058–66.
- [15] Yang CP, Liou GS, Jeng SH, Chen RS. *J Appl Polym Sci* 2002;86:2763–74.
- [16] Reddy DS, Chou CH, Shu CF, Lee GH. *Polymer* 2003;44:557–63.
- [17] Chuang KC, Scheiman DA, Fu J, Crawford M. *J Polym Sci Part A Polym Chem* 1999;37:2559–67.
- [18] Qiu ZM, Wang JH, Zhang QY, Zhang SB, Ding MX, Gao LX. *Polymer* 2006;47:8444–52.
- [19] Liu JG, He MH, Li ZX, Qian ZG, Wang FS, Yang SY. *J Polym Sci Part A Polym Chem* 2002;40:1572–82.
- [20] Liu Y, Xing Y, Zhang YH, Guan SW, Zhang HB, Wang Y, et al. *J Polym Sci Part A Polym Chem* 2010;48:3281–9.
- [21] Lin CH, Chang SL, Cheng PW. *Polymer* 2011;52:1249–55.
- [22] Guan Y, Wang DM, Song GL, Dang GD, Chen CH, Zhou HW, et al. *Polymer* 2014;55:3634–41.
- [23] Guan Y, Wang DM, Wang Z, Dang GD, Chen CH, Zhou HW, et al. *RSC Adv* 2014;4:50163–70.
- [24] Guan Y, Wang DM, Song GL, Dang GD, Chen CH, Zhou HW, et al. *High Perform Polym* 2014;26:455–62.
- [25] In I, Kim SY. *Polymer* 2006;47:547–52.
- [26] Shang YM, Fan L, Yang SY, Xie XF. *Eur Polym J* 2006;42:981–9.
- [27] Ando S, Matsuura T, Sasaki S. *Polym J* 1997;29:69–76.
- [28] You NH, Higashihara T, Ando S, Ueda M. *J Polym Sci Part A Polym Chem* 2010;48:656–62.
- [29] Hasegawa M, Sensui N, Shindo Y, Yokota R. *Macromolecules* 1999;32:387–96.
- [30] Li QX, Fang XZ, Wang Z, Gao LX, Ding MX. *J Polym Sci Part A Polym Chem* 2003;41:3249–60.